Available online at www.sciencedirect.com
ScienceDirect
Ceramics International 35 (2009) 259–264
CERAMICS INTERNATIONAL
www.elsevier.com/locate/ceramint

Synthesis and characterization of $MgAl_2O_4$–ZrO_2 composites

Ibram Ganesh [a,b], J.M.F. Ferreira [b,*]

[a] Centre for Advanced Ceramics, International Advanced Research Centre for Powder Metallurgy and New Materials (ARCI), Hyderabad 500005, AP, India
[b] Department of Ceramics and Glass Engineering, CICECO, University of Aveiro, P-3810-193 Aveiro, Portugal

Received 25 July 2007; received in revised form 15 September 2007; accepted 6 October 2007
Available online 10 January 2008

Abstract

Different types of dense 5–97% ZrO_2–$MgAl_2O_4$ composites have been prepared using a $MgAl_2O_4$ spinel obtained by calcining a stoichiometric mixture of aluminium tri-hydroxide and caustic MgO at 1300 °C for 1 h, and a commercial yttria partially stabilized zirconia (YPSZ) powder as starting raw materials by sintering at various temperatures ranging from 1500 to 1650 °C for 2 h. The characteristics of the $MgAl_2O_4$ spinel, the YPSZ powder and the various sintered products were determined by X-ray diffraction (XRD), scanning electron microscopy (SEM), BET surface area, particle size analysis, Archimedes principle, and Vickers indentation method. Characterization results revealed that the YPSZ addition increases the sintering ability, fracture toughness and hardness of $MgAl_2O_4$ spinel, whereas, the $MgAl_2O_4$ spinel hampered the sintering ability of YPSZ when sintered at elevated temperatures. A 20-wt.% YPSZ was found to be sufficient to increase the hardness and fracture toughness of $MgAl_2O_4$ spinel from 406 to 1314 Hv and 2.5 to 3.45 MPa $m^{1/2}$, respectively, when sintered at 1600 °C for 2 h.

Keywords: A. Sintering; C. Hardness; $MgAl_2O_4$ spinel; YPSZ; $MgAl_2O_4$–YPSZ composite; Fracture toughness

1. Introduction

Magnesium aluminate spinel ($MgAl_2O_4$) has received a great deal of attention as a technologically important material on account of its attractive properties such as high melting point (2135 °C), high chemical inertness, high thermal shock resistance, and low thermal expansion coefficient [1–5]. Owing to these properties, the $MgAl_2O_4$ has been extensively used for various purposes such as refractory material for cement rotary kilns and steel ladles [6–8], as a humidity sensor [9], and as a transparent ceramic material [10]. Further, the $MgAl_2O_4$ exhibits first deformation at 0.2 MPa and 2000 °C, does not react with SiO_2 until 1735 °C, with MgO or CaO until 2000 °C, with Al_2O_3 until 1924 °C, and it can be used for all the metals except alkaline earths [11]. Alkaline earth metals (M) react with Al_2O_3 in $MgAl_2O_4$ as these metals also tend to form M^{2+} ions like Mg. In spite of its high thermal shock resistance and chemical inertness, the $MgAl_2O_4$ spinel is not used in certain applications including molten metal filtrations because of its poor mechanical properties at room and high temperatures. In order to improve its mechanical properties, several approaches such as incorporation of secondary phase in the spinel matrix, retaining the sintered grain size below 100 nm by using nanocrystalline powders and altering the stoichiometry of $MgAl_2O_4$ composition, etc., have been tried [12–18]. However, the most successful approach has been the incorporation of partially stabilized tetragonal zirconia into the spinel matrix [13–17]. It is a known fact that the yttria partially stabilized zirconia (YPSZ) exhibits excellent mechanical properties and superior fracture toughness because of its unique phase transformations occurring over stress or temperature [18].

In a study, Fuzita et al. [12], have prepared a 20 wt.% ZrO_2–$MgAl_2O_4$ composite by hot pressing technique with a fracture toughness (K_{Ic}) of ~6.3 MPa $m^{1/2}$ and flexural strength of ~400 MPa. In another study, Hwang and Kim [13] have prepared a 10 wt.% zirconia/spinel composite with a relative density of ~98%, fracture toughness of ~12 MPa $m^{1/2}$ and strength of ~240 MPa from a pressed compact mixture of monoclinic zirconia (baddeleyite) and Mg–Al metal powder at 1550 °C for 3 h. Incidentally, all the existing routes for the preparation of ZrO_2–$MgAl_2O_4$ composites involve expensive raw materials and controlled processing steps. Therefore,

* Corresponding author. Tel.: +351 234 370242; fax: +351 234 370204.
E-mail address: jmf@ua.pt (J.M.F. Ferreira).

0272-8842/$34.00
doi:10.1016/j.ceramint.2007.10.006

products obtained by those methods can be used only for specialty applications and are not commercially viable for use in molten metal filter applications as their consumption is large in quantity. Nevertheless, the sinterability and mechanical properties of ZrO_2–$MgAl_2O_4$ composites prepared from YPSZ and $MgAl_2O_4$ spinel powder have not been studied thoroughly. Furthermore, there is a little information on the mechanical properties of ZrO_2 rich ZrO_2–$MgAl_2O_4$ composites in the literature [11–16].

In view of the above reasons, a systematic study was undertaken to prepare dense 5–97 wt.% YPSZ–$MgAl_2O_4$ composites using a stoichiometric $MgAl_2O_4$ spinel powder obtained from aluminium tri-hydroxide and caustic MgO at 1300 °C for 1 h and a commercially available YPSZ powder by sintering at different temperatures ranging from 1500 to 1650 °C for 2 h. All the sintered composites have been characterized by various spectroscopic and non-spectroscopic techniques in order to establish the effect of ZrO_2 on the sinterability and mechanical properties of $MgAl_2O_4$ ceramics.

2. Experimental procedure

2.1. Powder processing

The physico-chemical properties of aluminium tri-hydroxide (NALCO, NSPH-10, India), caustic MgO (Birla Periclase, India) and yttria partially stabilized zirconia (3YS, TOSOH, Japan) are given in Table 1. Stoichiometric dense $MgAl_2O_4$ spinel bodies were prepared according to the typical double stage firing process [19,20]. In a typical experiment, the required quantities of aluminum tri-hydroxide and caustic MgO were co-ground in a jar mill for 3–4 h. From the ground mixture, nodules were made using polyvinyl alcohol (PVA) solution (5 wt.%) followed by oven drying at 125 °C overnight. The dried nodules were calcined at 1300 °C for 1 h. The calcined spinel and YPSZ powders were separately vibro-milled in zirconia vessels to reduce their average particle sizes to 11.8 and 2.2 μm, respectively, using alumina and zirconia grinding media. The powders charge to balls ratio was maintained at 1:15 on weight basis. About 0.25 wt.% tri-ammonium citrate on the basis of powder weight was used as a dispersant in order to disperse the powder in the water.

Table 1
Physical properties and chemical composition of raw materials

Oxides present	$Al(OH)_3$	Caustic MgO	YPSZ
Minimum assay (wt.%)	–	–	>99.0
Al_2O_3 (wt.%)	64.5	–	0.005
MgO (wt.%)	–	82.86	–
$ZrO_2 + HfO_2$ (wt.%)	–	–	>94.0
Na_2O (wt.%)	0.3	0.093	0.004
CaO (wt.%)	0.03	0.908	–
SiO_2 (wt.%)	0.009	0.97	0.005
Fe_2O_3 (wt.%)	0.007	0.106	0.003
Y_2O_3 (wt.%)	–	–	5.17
LOI (RT-1000 °C)	34.5	15.5	0.44
Specific gravity (kg/m^3)	2420	3580	6020
Average particle size (μm)	85	5.22	0.49

Requisite quantities of ground spinel powder and YPSZ powder were mixed together to formulate different ZrO_2–$MgAl_2O_4$ composites and once again ground for another 15 min using vibro-mill. The ground and dried powders were converted into granules in the range of −30 to +100 BSS mesh (i.e., 149–595 μm) with the help of aqueous polyvinyl alcohol solution (5 wt.%). Dried granules were pressed uni-axially under a pressure of (200 MPa) into pellets having 20 mm diameter × 10 mm height. Pressed pellets were then sintered at 1500–1650 °C for 2 h.

2.2. Material characterization

The bulk density of the sintered materials was measured by the Archimedes principle [19,20]. Phase analysis of different samples was carried out by XRD (Bruker D8 advance system) using Cu Kα radiation. Relative phase composition of samples was calculated from the peak height measurements of the respective peaks [21]. Crystalline phases were identified by comparison with PDF-4 reference data from International Centre for Diffraction Data (ICDD). To obtain quantitative information of various phases, the most intense peak of each individual phase was taken into consideration. The peak heights of all the phases were summed up and the percentage concentration of a particular phase was estimated from the ratio of the strongest peak of that phase to the sum of various phases present in a given system [21]. The fraction of monoclinic zirconia (m-ZrO_2) in tetragonal and monoclinic mixtures was determined using the equation $\{Fm = (I_{t(1\,1\,1)})/(I_{m(1\,1\,1)} + I_{t(1\,1\,1)})\}$ [22]. Particle size distributions of all the powders used were measured using a particle size analyzer (Granulometer G 920, Cilas, France). The microstructure of dense spinel grains was examined by SEM (JSM–5410, JEOL, Japan) with an energy dispersive analysis with X-rays (Sigma 3.42 Quaser, Kevex, USA) for qualitative and quantitative analysis. Prior to SEM analysis all the samples were mounted on araldite platform, chemically etched (phosphoric acid at 185 ± 5 °C for 4 min), polished and gold coated for conductivity. The fracture toughness (K_{Ic}) values were calculated on the basis of the indentation method ($K_{Ic} = H a^{1/2} \times 0.203/(C/a)^{3/2}$) where a represents Vickers indent diagonal length, C the resulted crack length and H is a Vickers hardness (H_V = Kg/mm^2 = 10 MPa) [23]. Three to four samples were examined per case; in order to check the reproducibility of results and all the readings were averaged out and taken for consideration in the calculations [20].

3. Results and discussion

XRD patterns of the synthesized spinel powder and as received YPSZ powder are given in Fig. 1. As can be seen from Fig. 1, spinel powder obtained from a stoichiometric mixture of aluminium tri-hydroxide and caustic MgO at 1300 °C for 1 h shows XRD peaks mainly because of $MgAl_2O_4$ spinel phase (ICDD File No.: 00-021-1152) along with some minor peaks due to the un-reacted corundum (ICDD File No.: 00-046-1212) and periclase (ICDD File No.: 00-045-0946) phases. The

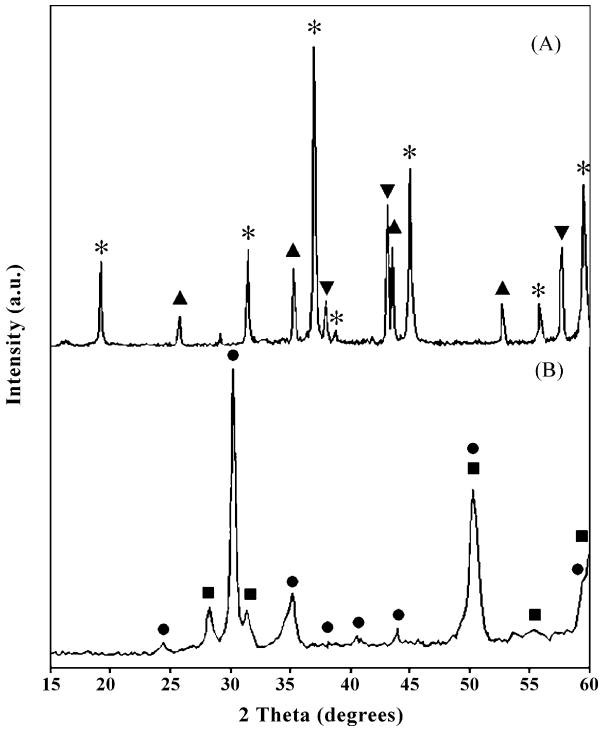

Fig. 1. XRD patterns of (A) spinel and (B) YPSZ powders: (*) $MgAl_2O_4$ spinel phase; (▲) α-Al_2O_3 corundum phase; (▼) MgO periclase phase; (●) t-ZrO_2, tetragonal zirconia phase; (■) m-ZrO_2, monoclinic zirconia phase.

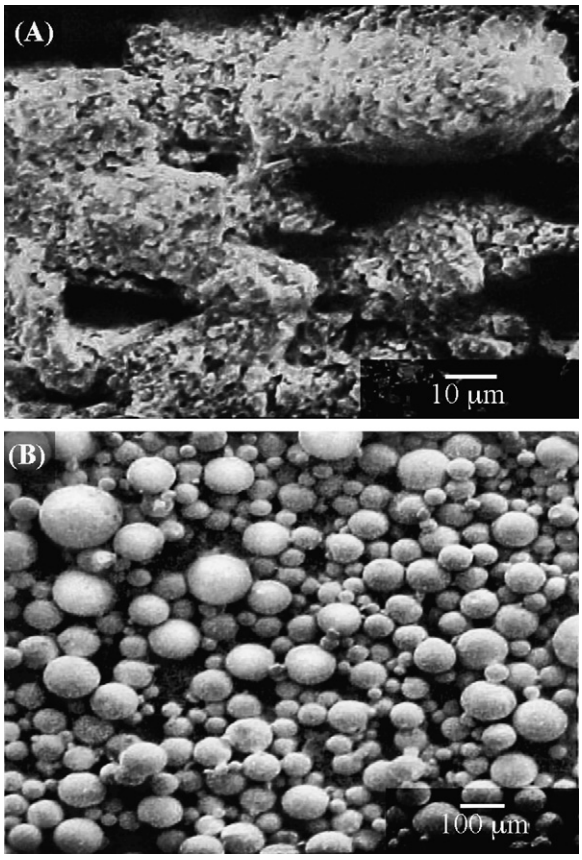

Fig. 2. SEM micrographs of (A) $MgAl_2O_4$ spinel and (B) YPSZ powders.

amount of spinel phase formed was estimated to be ~80%. As can be seen, the YPSZ powder shows XRD peaks primarily due to yttria stabilized tetragonal (ICDD File No.: 00-048-0224) and monoclinic (ICDD File No.: 00-037-1484) phases of zirconia with former being the major phase (~84%). The YPSZ powder contains ~5.4 wt.% yttria (claimed by the supplier). The SEM micrographs of ground spinel powder and as received YPSZ powder are given in Fig. 2(A) and (B), respectively. As can be seen, the as received YPSZ is a spray-dried powder consisting of granules in the range of 20–200 μm. Whereas, the ground $MgAl_2O_4$ spinel powder (Fig. 2(A)) still has some hard agglomerates like the one that was focused, consisting of very fine primary particles. The ground $MgAl_2O_4$ spinel powder consists of a wide particle size distribution, also denoting the presence of some remaining agglomerates, whereas the YPSZ powder consists of a very narrow particle size distribution (Fig. 3). It is a known fact that the smaller the particle size the larger would be its surface area and the high surface area powders normally exhibit higher reactivity, hence, improved sintering ability at elevated temperatures.

Table 2 lists the bulk density, fracture toughness, hardness, linear shrinkage, and the major XRD phase of $MgAl_2O_4$ spinel, 5–97 wt.% YPSZ–$MgAl_2O_4$ composites and pure YPSZ sintered at 1600 °C for 2 h. Their corresponding green density values are also presented in Table 2. For the purpose of clarity, different codes are given to the samples. As can be noted, the green density of composites increases gradually with the zirconia content. This is due to the fact that the theoretical density of Y_2O_3 partially stabilized TZP (6020 kg/m^3) is higher than the stoichiometric $MgAl_2O_4$ spinel (3580 kg/m^3). The $MgAl_2O_4$ spinel exhibited a bulk density value of ~3410 kg/m^3 (~95% of theoretical density) upon sintering at 1600 °C for 2 h. It has been noted in the previous paragraph that the compacted spinel powder consists of about 80% $MgAl_2O_4$ phase prior to sintering. It is well-documented in the literature that the partially spinelized (70–80%) powders possess higher reactivity during sintering when compared to fully spinelized or un-calcined powder at

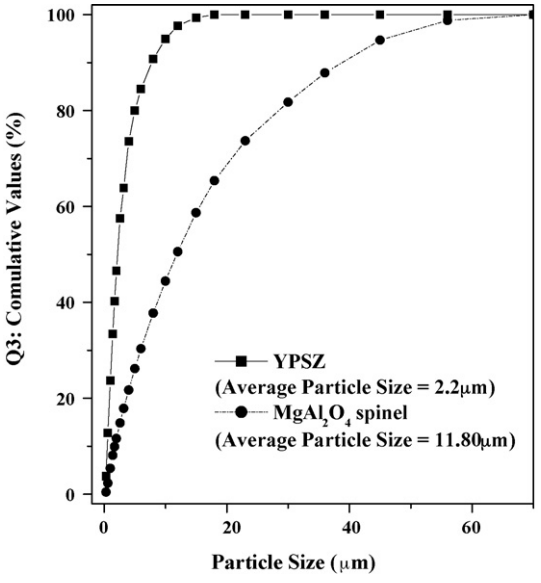

Fig. 3. Particle size distribution of $MgAl_2O_4$ spinel and YPSZ powders.

Table 2
Properties of various $MgAl_2O_4$–YPSZ composites sintered at 1600 °C for 2 h[†]

Sample	Composition	Green density (kg/m^3)	Bulk density (kg/m^3)	Relative density (%)	Theoretical density[‡] (kg/m^3)	Fracture toughness (MPa $m^{1/2}$)	Hardness (Hv)	Linear shrinkage (%)	Major XRD phase
S	$MgAl_2O_4$	2050 ± 14	3410 ± 17	95.20	3580	2.50 ± 03	406.42 ± 9	17.8	Spinel
S5Z	$MgAl_2O_4$–5 wt.% YPSZ	2160 ± 18	3570 ± 18	96.43	3702	2.51 ± 02	1220.64 ± 14	18.4	Spinel
S15Z	$MgAl_2O_4$–15 wt.% YPSZ	2130 ± 16	3630 ± 12	91.99	3946	2.53 ± 02	1257.14 ± 11	18.1	Spinel
S20Z	$MgAl_2O_4$–20 wt.% YPSZ	2140 ± 17	3750 ± 13	92.18	4068	3.45 ± 03	1314.60 ± 13	18.3	Spinel
S80Z	$MgAl_2O_4$–80 wt.% YPSZ	2840 ± 19	5240 ± 19	94.72	5532	4.03 ± 02	1402.44 ± 15	18.2	t-ZrO_2
S85Z	$MgAl_2O_4$–85 wt.% YPSZ	2910 ± 13	5360 ± 21	94.80	5654	4.45 ± 03	1326.34 ± 10	19.1	t-ZrO_2
S90Z	$MgAl_2O_4$–90 wt.% YPSZ	2980 ± 16	5430 ± 23	94.00	5776	4.48 ± 03	1293.18 ± 12	19.1	t-ZrO_2
S95Z	$MgAl_2O_4$–95 wt.% YPSZ	3160 ± 24	5640 ± 18	95.62	5898	5.36 ± 02	1295.40 ± 12	19.0	t-ZrO_2
S97Z	$MgAl_2O_4$–97 wt.% YPSZ	3180 ± 19	5680 ± 23	95.53	5946	6.63 ± 02	1355.08 ± 16	19.3	t-ZrO_2
Z	YPSZ	2970 ± 15	5880 ± 24	97.67	6020	6.98 ± 03	1386.76 ± 14	19.9	t-ZrO_2

[†] Values are arrived as described in Section 2.
[‡] These data was derived based on the rule of mixture of theoretical density of $MgAl_2O_4$ (3580 kg/m^3) and YPSZ (6020 kg/m^3).

elevated temperatures [20]. This is mainly because of the higher calcination temperatures required for complete spinelization than for partial spinelization, leading to the formation of hard agglomerates and less reactive powders [20]. The un-calcined powders cannot be sintered into a dense spinel body following single stage sintering process because of volume expansion associated with the spinel formation [24]. As expected, the bulk density of sintered YPSZ–$MgAl_2O_4$ composites increases with the YPSZ content (Fig. 4) as was observed in the case of green density values, irrespective of the sintering temperature used. However, a close look at relative density values (Table 2) reveals that adding a small amount of YPSZ (S5Z) improved the sinterability of $MgAl_2O_4$ spinel ceramics, decreasing it for further additions. However, in the case of zirconia rich YPSZ–$MgAl_2O_4$ composites, irrespective of $MgAl_2O_4$ spinel quantity their sintering ability has been decreased. The shrinkage values

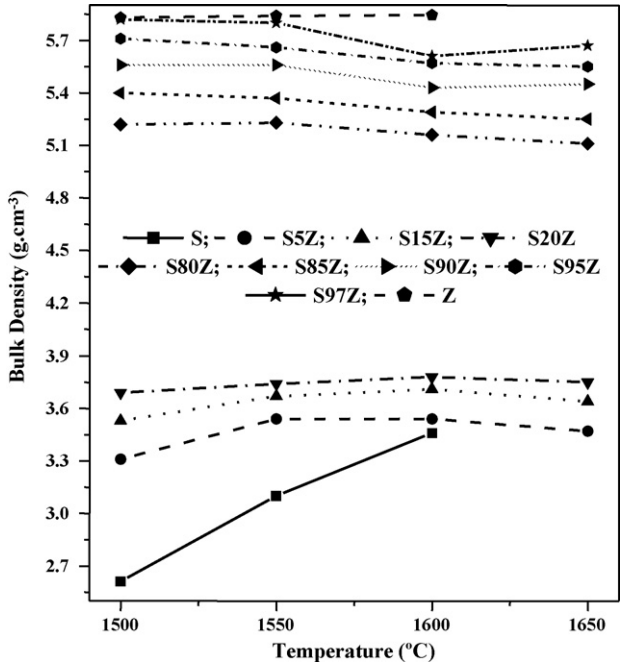

Fig. 4. Effect of sintering temperature on bulk density of various $MgAl_2O_4$–YPSZ composites sintered at temperatures 1500–1650 °C for 2 h.

(Table 2) listed for various composites substantiate the information obtained from their bulk density values. All YPSZ–$MgAl_2O_4$ composites exhibited apparent porosity and water absorption values almost close to zero when sintered at 1600 °C for 2 h.

The above results clearly suggest that the yttria partially stabilized zirconia is more sinterable as compared to stoichiometric $MgAl_2O_4$ spinel. Generally, a lower sintering temperature is always advantageous as it results in finer grain sizes of the constituents, which consequently improves metastable phase retention levels and strengths in the case of zirconia based materials. A close look at Fig. 4 also reveals that a gradual increase in bulk density values of spinel rich composites with sintering temperature up to 1600 °C, followed by a slight decrease with further increasing. In the case of zirconia rich composites, the maximum values can be noted even at 1548 °C, followed by a decreasing trend beyond this temperature. The decreasing bulk density of sintered materials beyond certain temperature is a well-known phenomenon related to the grain coarsening and pore coalescence.

It has been reported that ZrO_2 enhances the sinterability of $MgAl_2O_4$ spinels by accelerating the diffusion of O^{2-} ions [25]. According to Yamaguchi et al. [26], when ZrO_2 (m.p. ~2623 °C) is added to MgO (m.p. 2800 °C)/$MgAl_2O_4$ spinel (m.p. 2135 °C) composite, Zr^{4+} goes into MgO lattice (the ionic radii of Zr^{4+} is 7.2×10^{-9} m (0.72 Å), Mg^{2+} is 7.2×10^{-9} m (0.72 Å)) forming a solid solution ZrO_2–MgO, creating magnesium ion vacancies in MgO crystals, and thus generated vacancies accelerate the diffusion of O^{2-} ions to form dense products at >1500 °C. Further, ZrO_2 is also known to accelerate the oxygen ion diffusion thereby the sintering ability of the materials [27]. The same mechanism may be applicable in the present systems too. Another possible reason for improved sintering ability of $MgAl_2O_4$ spinel in the presence of ZrO_2 is that when ZrO_2 is added to MgO based materials, ZrO_2 mostly exists at grain boundaries during sintering and controls grain growth thereby promotes the sintering process by accelerating oxygen ion diffusion through the grain boundaries.

As can be observed from fracture toughness and hardness values (Table 2), in general, the zirconia rich composites (i.e.,

S80Z–S97Z samples) exhibited higher fracture toughness and hardness as compared to spinel rich composites. The results presented in Table 2 also reveal that irrespective of the sintered density the YPSZ increases the fracture toughness and hardness of $MgAl_2O_4$ spinel. Though, the improvement in the case of fracture toughness is not so high but it is very significant in the case of hardness. The improved fracture toughness of $MgAl_2O_4$ by the incorporation of ZrO_2 is due to a combination of several toughening mechanisms including stress-induced t → m phase transformation toughening, microcrack toughening and crack deflection. When ZrO_2 is finely dispersed in the matrix of $MgAl_2O_4$ it exists in the form of tetragonal crystals that are meta-stable at room temperature. This meta-stable t-ZrO_2 transforms to m-ZrO_2 by shear stress-induced during fracture (stress-induced transformation). This tetragonal–monoclinic transformation is accompanied by volume expansion, which nucleate microcracks in the surrounding material and restrains the propagation of fracture. Quenard et al. [28] also made a similar observation in their recent study of zirconia–spinel composites prepared from combustion synthesized powders. However, in the case of zirconia rich composites, both fracture toughness and hardness values are decreased with spinel addition. Interestingly, this decrease is less in the case of hardness when compared to fracture toughness values.

Examples of SEM micrographs of $MgAl_2O_4$–97% ZrO_2 and $MgAl_2O_4$–85% ZrO_2 (S85Z) compacts sintered at 1600 °C for 2 h are shown in Fig. 5(A) and (B), respectively, wherein the brighter portions correspond to ZrO_2 and darker zones are correspond to $MgAl_2O_4$ phase and porosity. The microstructures of the other samples presented similar features, but with the dark portions increasing with the enrichment of the compositions in $MgAl_2O_4$ spinel phase.

X-ray diffraction patterns of Z, S95Z, S80Z, S20Z, S5Z and S sample sintered at 1600 °C for 2 h are given in Fig. 6. As can be seen from this figure, the S sample shows only XRD peaks of $MgAl_2O_4$ spinel phase (ICDD File No.: 00-021-1152). The XRD peaks corresponding to corundum (ICDD File No.: 00-046-1212) and periclase (ICDD File No.: 00-045-0946) as observed in the calcined powder (Fig. 1) have totally disappeared after sintering. This is due to the fact that according to the phase diagram of binary MgO–Al_2O_3, $MgAl_2O_4$ is the only phase formed at temperatures up to 1600 °C [1–5]. At this temperature, the solid solubility of MgO and Al_2O_3 in the spinel is 2% and 6%, respectively [1–5,19]. On increasing the firing temperature to 1700 °C, the solubility in the spinel increases to 3% and 10%, respectively [19]. Thus, even if any small variation in the stoichiometry of $MgAl_2O_4$ spinel is present, it does not show XRD peaks due to periclase and corundum phases after sintering at 1600 °C for 2 h. These results are well-comparable with the data reported elsewhere [19,20]. The pure sintered YPSZ shows XRD peaks only due to tetragonal ZrO_2 (ICDD File No: 00-048-0224) phase. Further, a gradual increase in the intensity of XRD peaks of $MgAl_2O_4$ and a concomitant decrease of XRD peaks' intensity of t-ZrO_2 is noted with increasing added amounts of spinel to the zirconia matrix. The presence of tetragonal ZrO_2 phase in the YPSZ–

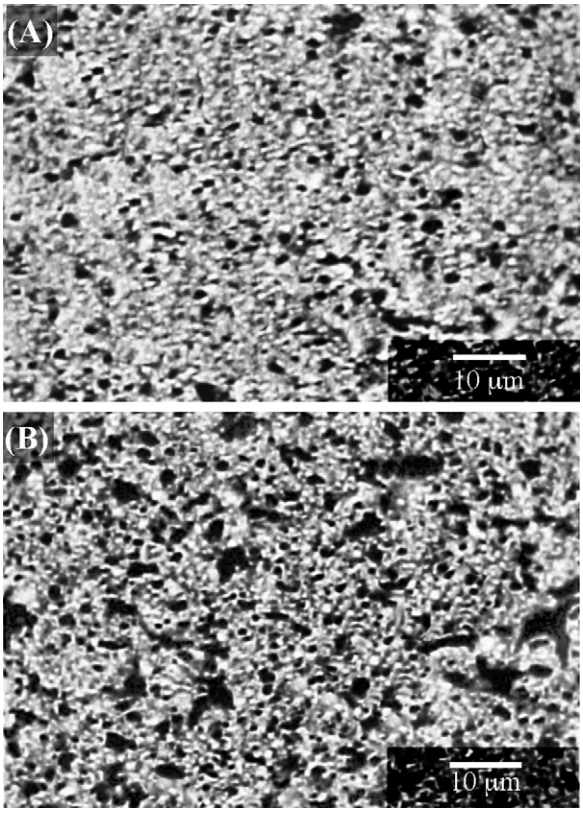

Fig. 5. SEM of (A) $MgAl_2O_4$–97% YPSZ and (B) $MgAl_2O_4$–85% YPSZ composites sintered at 1600 °C for 2 h.

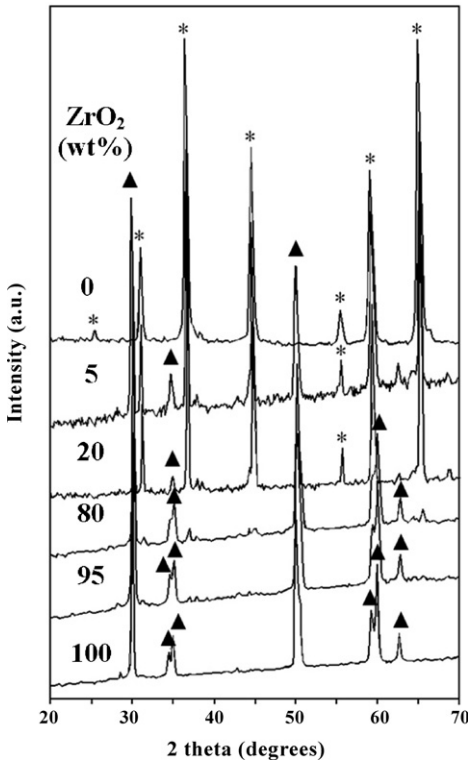

Fig. 6. XRD patterns of different $MgAl_2O_4$–YPSZ composites sintered at 1600 °C for 2 h: (*) $MgAl_2O_4$ spinel phase; (▲) tetragonal zirconia phase, t-ZrO_2.

$MgAl_2O_4$ composites is responsible for their high fracture toughness and hardness values.

4. Conclusions

The following conclusions can be drawn from the above study:

(1) A stoichiometric $MgAl_2O_4$ spinel with a theoretical density of greater than 95%, hardness of ~406 Hv and a fracture toughness of ~2.50 MPa $m^{1/2}$ could be prepared following a conventional double stage sintering process at 1600 °C for 2 h from a spinel powder having a average particle size < 11.8 μm, a compact (green) density > 2005 kg/m^3, and the spinel content > 80%.
(2) The yttria partially stabilized zirconia exhibited a theoretical density > 97%, a fracture toughness of ~7 MPa $m^{1/2}$ and hardness of 1386 Hv when sintered at 1600 °C for 2 h.
(3) The bulk density, hardness and fracture toughness (~3410 kg/m^3, ~406.42 Hv and ~2.50 MPa $m^{1/2}$) of $MgAl_2O_4$ spinel could be improved to ~3705 kg/m^3, ~1314 Hv and ~3.45 MPa $m^{1/2}$, respectively, by adding 20 wt.% YPSZ and sintering at 1600 °C for 2 h.
(4) Addition of 5 wt.% $MgAl_2O_4$ spinel decreased the fracture toughness and hardness of YPSZ from 7 to 5.4 MPa $m^{1/2}$ and from 1386 to 1295 Hv, respectively, when sintered at 1600 °C for 2 h.

Acknowledgments

IG thanks SERC-DST, Government of India, for awarding BOYSCAST Fellowship (SR/BY/E-04/06). The financial support of CICECO is also acknowledged.

References

[1] C. Baudin, R. Martinez, P. Pena, High-temperature mechanical behaviour of stoichiometric magnesium spinel, J. Am. Ceram. Soc. 78 (7) (1995) 1857–1862.
[2] W.T. Baker, J.G. Lindsay, Reactive magnesia spinel, preparation and properties, Am. Ceram. Soc. Bull. 46 (11) (1967) 1094–1097.
[3] J.T. Baitley, R. Russel Jr., Sintered spinel ceramics, in: Presented at the 69th Annual Meeting of the American Ceramic Society, New York, NY, May 3, 1967.
[4] E. Ruh, The refractory industry today—Japan and the United States, Am. Ceram. Soc. Bull. 63 (9) (1984) 1140–1142.
[5] I. Ganesh, S. Bhattacharjee, B.P. Saha, R. Johnson, K. Rajeshwari, R. Sengupta, M.V. Ramanarao, Y.R. Mahajan, An efficient $MgAl_2O_4$ spinel additive for improved slag erosion and penetration resistance of High-Al_2O_3 and MgO–C refractories, Ceram. Int. 28 (2002) 245–253.
[6] J. Mori, W. Watenabe, M. Yoshimura, Y. Oguchi, T. Kawakami, Materials design of monolithic refractories for steel ladle, Bull. Am. Ceram. Soc. 69 (7) (1990) 1172–1176.
[7] B. Ghosh, P. Chakrabarty, P.G. Pal, S.K. Mitra, K.S. Swaminathan, Magnesio-aluminate spinel—a potential raw material for making new generation refractories, in: Proc. UNITESR'95, 1995, 541–549.
[8] G.E. Gonsalves, A.K. Duarte, P.O.R.C. Brant, Magnesia-spinel brick for cement rotary kilns, Bull. Am. Ceram. Soc. 72 (2) (1993) 49–54.
[9] Y. Shimizu, H. Arai, T. Seiyama, Theoretical studies on the impedance-humidity characteristics of ceramic humidity sensors, Sens. Actuators 7 (1985) 11–22.
[10] L. Ji-Guang, T. Ikegami, L. Jong-Heum, T. Mori, Fabrication of translucent magnesium aluminate spinel ceramics, J. Am. Ceram. Soc. 83 (11) (2000) 2866–2868.
[11] J.H. Belding, E.A. Letzgus, Process for producing magnesium aluminate spinel, U.S. Patent No. 3,950,504, 13th April, 1976.
[12] M. Fuzita, H. Martinez, A. Osaka, Y. Miura, Am. Ceram. Soc. Bull. 103 (1995) 825–830.
[13] K.H. Hwang, S.M. Kim, J. Korean Ceram. Soc. 33 (7) (1996) 779.
[14] A. Addad, J. Crampon, R. Guinebretiere, A. Dauger, R. Duclos, Grain boundary sliding-induced deformation in a 30 wt% zirconia–spinel composite: influence of stress, J. Euro. Ceram. Soc. 20 (2000) 2063–2068.
[15] O. Quenard, C.H. Laurent, A. Peigney, A. Rousset, Zirconia–spinel composites. Part II: mechanical properties, Mater. Res. Bull. 35 (2000) 1979–1987.
[16] I. Ganesh, B. Srinivas, R. Johnson, G.V.N. Rao, Y.R. Mahajan, Effect of method of preparation on sinterability and properties of nanocrystalline $MgAl_2O_4$ and ZrO_2–$MgAl_2O_4$ materials, Br. Ceram. Trans. 102 (3) (2003) 119–128.
[17] S. Bhaduri, S.B. Bhaduri, Microstructural and mechanical properties of nanocrystalline spinel and related composites, Ceram. Int. 28 (2002) 153–158.
[18] N. Claussen, Advances in ceramics, in: N. Claussen, M. Ruhle, A.H. Heuer (Eds.), Science and Technology of Zirconia II, vol. 12, The American Ceramic Society, Columbus, Ohio, 1984„ p. 235and references therein.
[19] I. Ganesh, K.A. Teja, N. Thiyagarajan, R. Johnson, B.M. Reddy, Formation and densification behaviour of magnesium aluminate spinel: the influence of CaO and moisture in the precursors, J. Am. Ceram. Soc. 88 (10) (2005) 2752–2761, and references therein.
[20] I. Ganesh, S. Bhattacharjee, B.P. Saha, R. Johnson, Y.R. Mahajan, A new sintering aid for magnesium aluminate spinel, Ceram. Int. 27 (7) (2001) 773–779, and references therein.
[21] B.D. Cullity, Elements of XRD, second ed., Addison, Wesley, Reading MA, 1978.
[22] R.G. Garvie, P.S. Nicholson, J. Am. Ceram. Soc. 55 (6) (1972) 303.
[23] I.-L. Ekberg, R. Lundberg, R. Warren, R. Carlson, in: A.M. Brandt, I.H. Marshall (Eds.), British Matrix Composites, vol. 2, Elsevier Applied Science, 1998.
[24] Z.E. Nakagawa, N. Enomoto, I.S. Yi, K. Asano, Effect of corundum/periclase sizes on the expansion behavior during synthesis of spinel, in: Proc. Unitecer, 1995, Congress, Tokyo, (1995), pp. 379–386.
[25] T. Suzuki, K. Itatani, M. Aizawa, F. Scott Howell, A. Kishioka, Sinterability of spinel ($MgAl_2O_4$)-zirconia composite powder prepared by double nozzle ultrasonic spray pyrolysis, J. Eur. Ceram. Soc. 16 (1996) 1171–1178.
[26] G. Yamaguchi, M. Nakano, R. Ychimura, Yogyo-Kyokai-shi 79 (1971) 140–145.
[27] H.W. Walter, W.S. Thomas, Chemical preparation of zirconium–aluminum–magnesium oxide composites, US patent No. 4880757, Nov. 14th, 1989.
[28] O. Quenard, C. Laurent, A. Peigney, A. Rousset, Zirconia–spinel composites, part II: mechanical properties, Mater. Res. Bull. 35 (12) (2000) 1979–1987.